minerals

MDPI

Article

Anti-Aliasing and Anti-Leakage Frequency–Wavenumber Filtering Method for Linear Noise Suppression in Irregular Coarse Seismic Data

Shengqiang Mu [1,2], Liang Huang [1,2], Liying Ren [3], Guoxu Shu [4] and Xueliang Li [1,2,*]

[1] State Key Laboratory of Deep Petroleum Intelligent Exploration and Development, Institute of Geology and Geophysics, Chinese Academy of Sciences, Beijing 100029, China; mushengqiang20@mails.ucas.ac.cn (S.M.); huangliang16@mails.ucas.ac.cn (L.H.)
[2] University of Chinese Academy of Sciences, Beijing 100049, China
[3] Liaohe Geophysical Exploration Company of BGP CNPC, Panjin 124010, China; rly110214@163.com
[4] School of Geophysics and Information Technology, China University of Geoscience (Beijing), Beijing 100083, China; gxushu@163.com
* Correspondence: lixl0@163.com

Abstract: Linear noise, a significant type of interference in exploration seismic data, adversely affects the signal-to-noise ratio (SNR) and imaging resolution. As seismic exploration advances, the constraints of the acquisition environment hinder the ability to acquire seismic data in a regular and dense manner, complicating the suppression of linear noise. To address this challenge, we have developed an anti-aliasing and anti-leakage frequency–wavenumber (f-k) filtering method. This approach effectively mitigates issues of spatial aliasing and spectral leakage caused by irregular coarse data acquisition by integrating linear moveout correction and anti-leakage Fourier transform into traditional f-k filtering. The efficacy of our method was demonstrated through examples of linear noise suppression on both irregular coarse synthetic data and field seismic data.

Keywords: linear moveout correction; anti-leakage Fourier transform; f-k filtering; linear noise; irregular coarse acquisition

check for updates

Academic Editor: Luigi Jovane

Received: 27 December 2024
Revised: 19 January 2025
Accepted: 21 January 2025
Published: 23 January 2025

Citation: Mu, S.; Huang, L.; Ren, L.; Shu, G.; Li, X. Anti-Aliasing and Anti-Leakage Frequency–Wavenumber Filtering Method for Linear Noise Suppression in Irregular Coarse Seismic Data. *Minerals* **2025**, *15*, 107. https://doi.org/10.3390/min15020107

Copyright: © 2025 by the authors. Licensee MDPI, Basel, Switzerland. This article is an open access article distributed under the terms and conditions of the Creative Commons Attribution (CC BY) license (https://creativecommons.org/licenses/by/4.0/).

1. Introduction

Seismic exploration is one of the most effective geophysical methods for revealing the structure of the earth's crust and detecting oil and minerals [1–4]. However, during the acquisition of seismic data, environmental complexities often lead to significant noise contamination. Noise suppression processing is a crucial aspect of seismic data processing [5]. Among various types of noise, linear noise is a primary interference wave encountered during seismic data acquisition. Linear noise is a type of coherent noise characterized by distinct kinematic properties and frequencies similar to those of valid reflection waves. It propagates along the spatial or temporal axis in a linear pattern within seismic records, with its apparent velocity remaining constant or exhibiting linear variation. In the frequency–wavenumber (f-k) domain, it typically appears as an energy band with a specific slope [6–8]. This category includes guided waves, body waves, surface waves, and strong sound waves, all of which manifest as linear events in the data. Seismic-guided waves are generated by subsurface layer interfaces or heterogeneous media, typically propagating along specific paths through reflection, refraction, or mode conversion. Body waves, during propagation, can be mixed with other noise sources (such as equipment interference or traffic), resulting in body wave noise with linear characteristics. Seismic waves traveling along the surface

generate surface waves with a fixed apparent velocity, induced by the surface medium (such as loose soil layers or rock layers). Strong sound waves are primarily caused by mechanical vibrations from seismic instruments, ground vibrations, or external disturbances (such as construction noise or traffic). Linear noise can severely degrade effective reflection signals, significantly lowering the signal-to-noise ratio (SNR) of seismic data [9]. Additionally, high-angle linear noise can appear on stacking profiles, obscuring the true orientation of geological strata and complicating the identification of fault systems, ultimately impacting the quality of final imaging [10].

Various techniques have been developed to attenuate linear noise in seismic exploration, including frequency–wavenumber (f-k) filtering, f-x filtering, radial trace (RT) filtering, and τ-p transform filtering. Embree et al. verified that f-k filtering can effectively remove regular, un-aliased linear noise [11]. Guo et al. introduced an f-x domain operator extrapolation technique, leveraging the relationship between frequency and trace moveout to suppress both random and linear noise [12]. Liu proposed Karhunen–Loève (KL) transform to model and subtract ground roll from original data [13]. Henly utilized RT transform to suppress linear feature signals [14]. Zhu et al. combined local RT transform with a step-varying median filter to effectively eliminate coherent linear noise in prestack seismic data, which is called local radial trace median filter (LRMF) [15]. Lu et al. proposed polynomial approximation for suppressing local linear coherent noise [16]. Hong et al. advanced the beamforming filtering method, yielding improved denoising performance over traditional techniques [17]. Neelamani et al. and Tong et al. employed Curvelet transform for coherent linear noise attenuation [18,19]. Qin and Teng et al. demonstrated significant results using wavelet frequency division characteristics for linear noise suppression in actual seismic data processing [20,21]. Additionally, multiple radon transformations have been used to exploit the distinguishability of effective and unwanted signals in the τ-p domain [22,23]. Mathematical morphological filtering (MMF) has shown success in suppressing linear noise in both synthetic and field seismic data [7]. In recent years, artificial intelligence has developed rapidly and has gained widespread attention and application in seismic data denoising, with significant potential for further development [24–26].

As seismic exploration research progresses, the exploration environment has grown increasingly complex. Obstacles such as villages, ponds, and roads hinder seismic data acquisition according to the regular seismic geometry system for shot and receiver points [27,28]. Irregular sampling can adversely affect the Fourier spectrum of seismic data, leading to a phenomenon known as spectrum leakage, where energy from one Fourier coefficient leaks onto others [29–32]. Spectral leakage poses significant challenges to various seismic data processing methods, including noise suppression and data reconstruction [33]. Furthermore, during seismic data acquisition, the spatial sampling density should comply with the requirements of Kotelnikov's theorem, meaning that the spatial sampling rate must be at least twice the maximum wavenumber. However, constraints from surface obstacles or economic considerations may result in seismic data that do not meet this criterion, leading to varying degrees of spatial aliasing in the wavenumber domain [6]. The combined effects of spatial aliasing and spectral leakage complicate the suppression of linear noise, rendering many of the previously mentioned techniques less effective in achieving satisfactory processing results. For the linear noise suppression of irregular coarse seismic data acquired in complex survey areas, traditional linear noise suppression methods, due to the limitations of their underlying principles, are unable to address spectral leakage and spatial aliasing issues, resulting in unsatisfactory linear noise suppression performance. In this context, we have innovatively proposed, for the first time, a method for linear noise suppression in irregular coarse seismic data. In this work, we integrate linear moveout correction and anti-leakage Fourier transform into the traditional f-k filtering approach.

The linear moveout correction addresses spatial aliasing caused by undersampling, while the anti-leakage Fourier transform reduces the spectral leakage effects associated with irregular acquisition. As a result, we have developed a linear noise suppression technique specifically designed to tackle the spatial aliasing and spectral leakage issues inherent in irregular and coarse acquisition. The remainder of the paper is organized as follows. In the section titled "Theory and methods", we detail the linear moveout correction, anti-leakage Fourier transform, and anti-aliasing and anti-leakage f-k filtering method. In the subsequent "Application" section, we validate the effectiveness of our linear noise suppression technique using synthetic seismic data as well as field seismic data.

2. Theory and Methods

2.1. Linear Moveout Correction

During the acquisition of field seismic data, budget constraints and environmental factors often prevent the spatial sampling rate from meeting the requirements of the sampling theorem, leading to spatial aliasing in the f-k domain. In traditional f-k filtering, linear noise associated with the aliased spectral components cannot be effectively suppressed, significantly diminishing the overall noise suppression performance. A practical solution to this issue is to apply linear moveout correction to the data prior to noise suppression, which shifts unwanted signals to lower dips and effectively mitigates the effects of spatial aliasing. The process of applying linear moveout correction based on the following formula:

$$T = \mathrm{X}/V, \tag{1}$$

where T is the static time shifts, X is the offset, and V is the linear moveout correction velocity.

To demonstrate the effectiveness of linear moveout correction in eliminating spatial aliasing, we simulated three linear noises with apparent velocities of 100 m/s, 150 m/s, and 200 m/s along the survey line, using spatial sampling intervals of 5 m. The synthesized linear noise and its spectrum are shown in Figure 1. The linear noise corresponding to 100 m/s exhibits severe spectrum aliasing, while the linear noise corresponding to 150 m/s exhibits slight spectrum aliasing. In contrast, the linear noise corresponding to 200 m/s does not exhibit spectrum aliasing and can be easily removed using f-k filtering method. Consequently, for low-apparent-velocity noise, directly removing it from the f-k spectrum proves challenging due to insufficient spatial sampling. We applied linear moveout correction on the data at a velocity of 270 m/s, with results presented in Figure 2. We observe that the linear moveout correction reduces the inclination angle of the linear noise and eliminates spectral aliasing, allowing for effective suppression in the f-k spectrum.

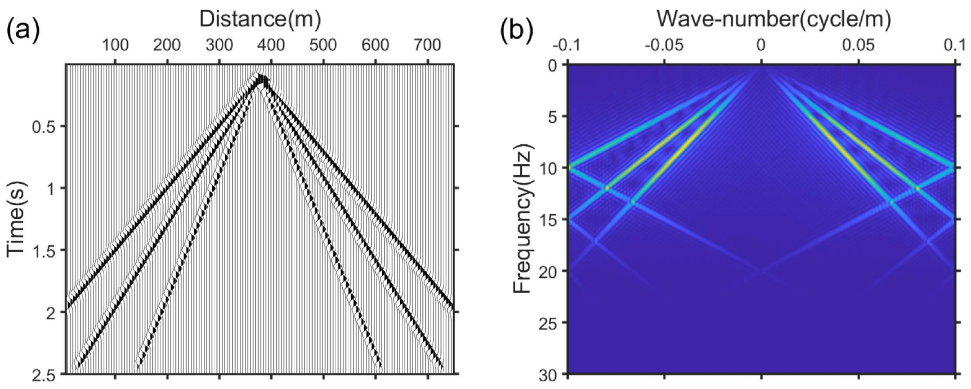


Figure 1. Synthetic regular linear noise (**a**) and its f-k spectrum (**b**).

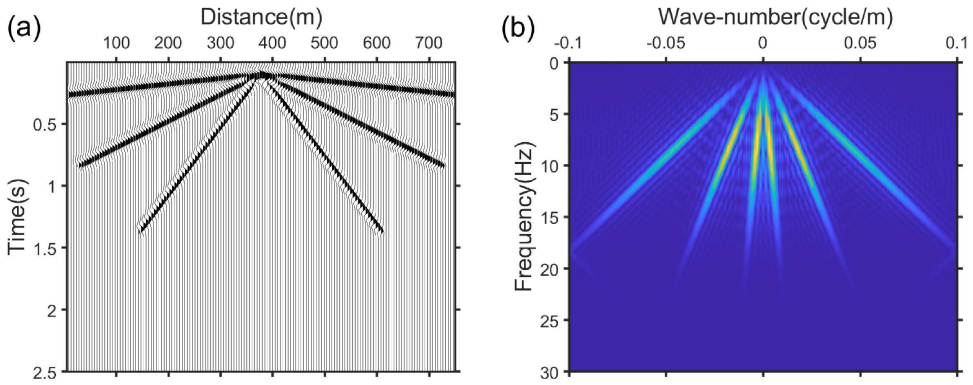


Figure 2. Synthetic regular linear noise after LMO correction (**a**) and its f-k spectrum (**b**).

2.2. Anti-Leakage Fourier Transform

As seismic exploration continues to advance, the field acquisition environment has become increasingly complex, such as mountains, lakes, rivers, etc. This complexity makes it difficult to arrange shot and receiver points in a regular manner, resulting in irregular seismic data that pose additional challenges for data processing.

For acquired irregular seismic data, the associated Fourier coefficients in the f-k domain can be computed via nonuniform discrete Fourier transform (NDFT) [34]

$$D(m\Delta k, w) = \sum_{n=0}^{N-1} d(x_n, w) e^{im\Delta k x_n} \Delta x_n, \quad (2)$$

where $\Delta k = 2\pi/(x_{N-1} - x_0)$, m is the wavenumber index, and Δx_n indicates the spacing between consecutive traces. Compared to regular sampling, irregularly sampled data produce a noticeable effect in the f-k spectrum, which is known as spectral leakage, where energy from one Fourier coefficient leaks into others. To further illustrate the spectral leakage effect, we performed irregular sampling on the linear signals simulated in the previous section, using an average interval of 5 m between sampling points. Figures 3 and 4 display the irregular linear signals and their spectra before and after linear moveout correction. It is evident that, compared to regular sampling, irregular sampling causes the energy of Fourier coefficients to leak across the entire f-k spectrum, creating additional challenges for f-k filtering.

To obtain the true spectrum of irregular seismic data without spectral leakage, Xu et al. proposed the anti-leakage Fourier transform algorithm [30]. This method iteratively constructs the Fourier coefficients by searching for the element with maximum amplitude and subtracting the associated component from the original seismic data until all the significant Fourier coefficients are estimated. The process includes the following steps:

(1) Compute the f-k spectrum of the irregular data;
(2) Select the strongest Fourier component and add this value to the estimated spectrum;
(3) Subtract the contribution of this Fourier component from the input data;
(4) Input the updated Fourier component into step (2) until the desired number of Fourier components is reached or the data residual is small enough.

For the irregular linear signal corrected by linear moveout correction, we applied the anti-leakage Fourier transform algorithm to obtain its true spectrum. Figure 5 displays the reconstructed regular linear signal along with its spectrum. It is evident that the spectral leakage caused by irregular acquisition has been effectively addressed. Therefore, the combination of linear moveout correction and anti-leakage Fourier transform can effectively solve the issues of spatial aliasing and spectral leakage resulting from irregular coarse acquisition.

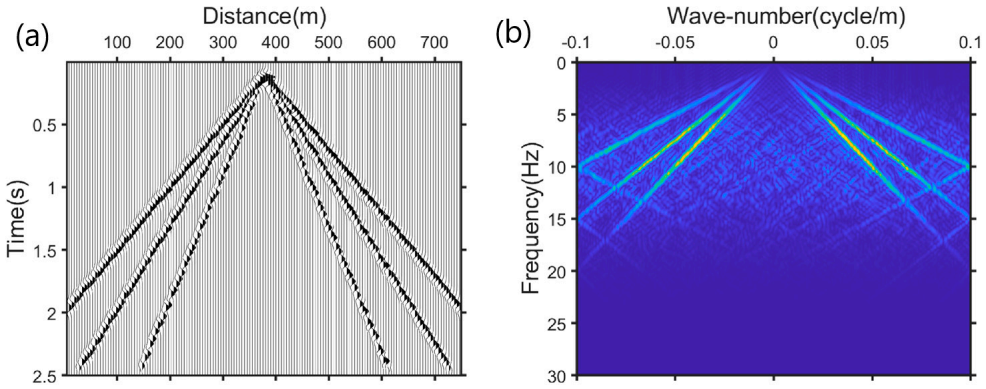


Figure 3. Synthetic irregular linear noise (**a**) and its f-k spectrum (**b**).

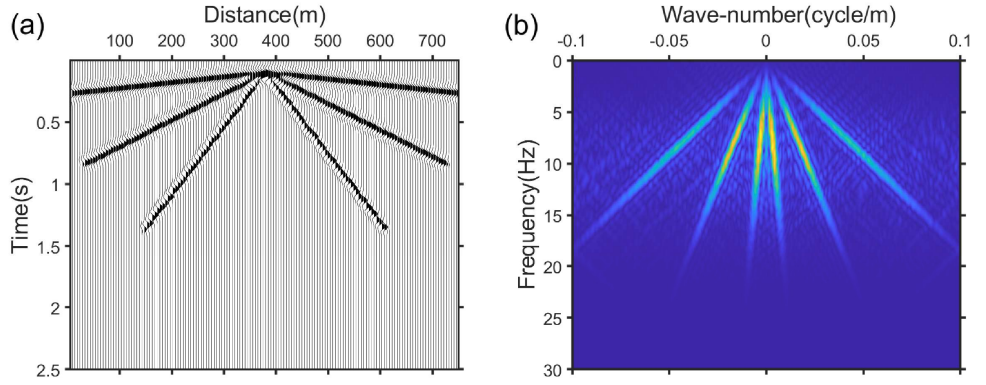


Figure 4. Synthetic irregular linear noise after linear moveout correction (**a**) and its f-k spectrum (**b**).

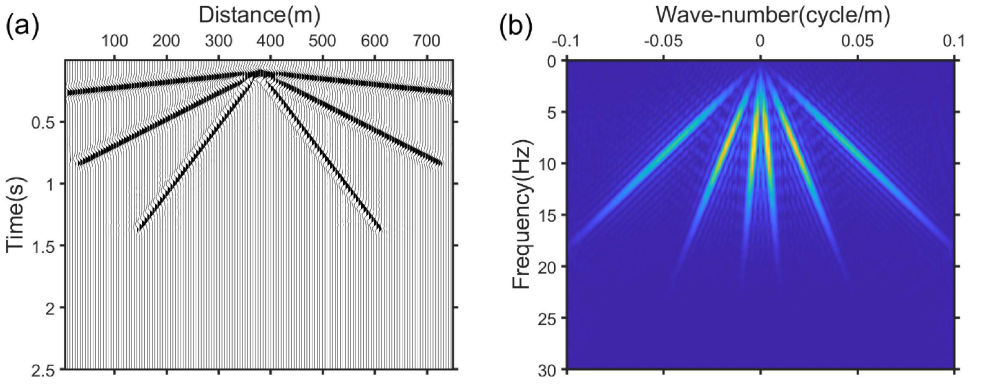


Figure 5. Synthetic irregular linear noise after linear moveout correction (**a**) and its anti-leakage Fourier transform spectrum (**b**).

2.3. Anti-Leakage and Anti-Aliasing f-k Filtering

The f-k filtering method, based on two-dimensional Fourier transform, is also known as apparent velocity filtering. This technique leverages the differences in apparent velocity between unwanted noise and the signal to distinguish them in the f-k domain, enabling the removal of undesired energy from the original data. The f-k filtering equation in the f-k domain can be expressed as follows:

$$\widetilde{D}(k,w) = D(k,w)\cdot H(k,w), \tag{3}$$

where $H(k,w)$ is the designed filter and satisfies the following conditions:

$$H(k,w) = \begin{cases} 0, \ (f,k) \in suppression\ regin \\ 1, \ (f,k) \in \ \ effective \ \ \ regin \end{cases}, \tag{4}$$

The traditional f-k filtering method effectively suppresses linear noise in regular high-density seismic data. However, it struggles to achieve optimal noise suppression in irregular coarse acquisition data due to its theoretical limitations.

As mentioned earlier, linear moveout correction can mitigate the effects of spatial aliasing, while anti-leakage Fourier transform addresses spectral leakage caused by irregularities and provides the true f-k spectrum. Therefore, we combine linear moveout correction, anti-leakage Fourier transform, and the traditional f-k filtering method to develop an anti-aliasing and anti-leakage f-k filtering method. The steps of the anti-aliasing and anti-leakage f-k filtering method can be summarized as follows:

1. Obtain the irregular coarse seismic data and the apparent velocity of unwanted linear noise;
2. Select the appropriate velocity and apply linear moveout correction;
3. Use the anti-leakage Fourier transform algorithm to obtain the true f-k spectrum;
4. Identify the suppression region of the f-k spectrum based on the apparent velocity of unwanted linear noise;
5. Retrieve the denoised seismic data using inversion FFT;
6. Output the final denoised seismic data by applying reverse linear moveout correction.

It is important to note that the linear noise suppression method for irregular coarse seismic data proposed in this paper can only partially address spatial aliasing. It cannot completely resolve severe cases of spatial aliasing. Moreover, for seismic events without spatial aliasing, spatial aliasing may occur after linear moveout correction, which could affect the subsequent true f-k spectrum calculation based on anti-leakage Fourier transform and the effective signal reconstruction. Therefore, comprehensive data analysis and parameter design should be conducted before noise suppression.

To help the readers better understand how anti-aliasing and anti-leakage f-k filtering works, we give a demonstration in Figure 6 that corresponds to the aforementioned.

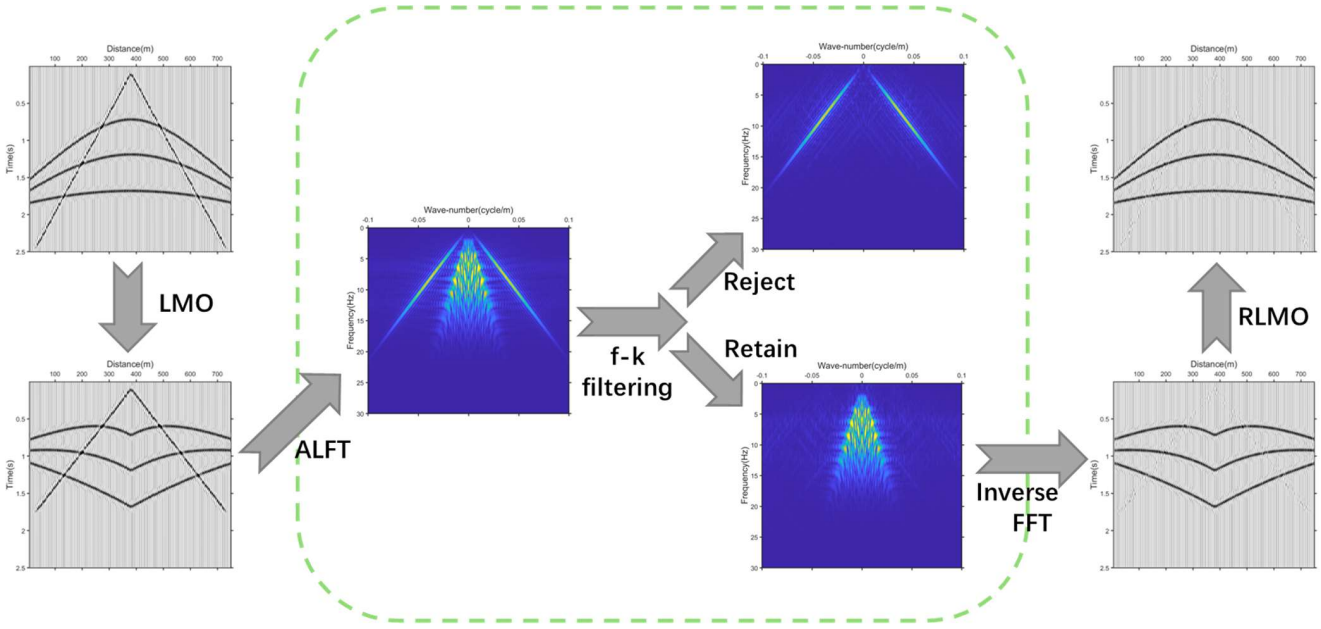


Figure 6. Workflow of the anti-aliasing and anti-leakage f-k filtering method.

3. Applications

3.1. Simple Synthetic Data

We first tested the proposed anti-aliasing and anti-leakage f-k filtering method on a synthetic example. The data consist of three primaries and three linear noises with apparent velocities of 100 m/s, 150 m/s and 200 m/s, respectively. The sampling points are irregularly distributed, with an average sampling interval of 5 m. The test data and their f-k spectrum are shown in Figure 7.

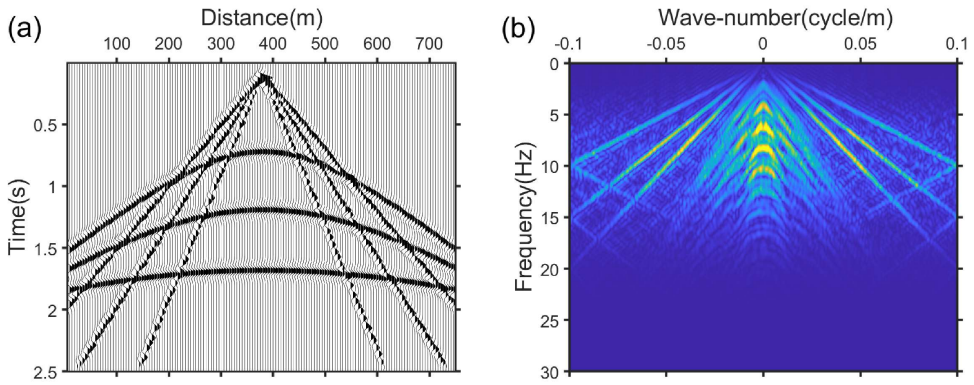


Figure 7. Synthetic irregular seismic data consisting of three types of linear noise, three primaries (**a**), and the f-k spectrum (**b**).

As observed, the irregular distribution of sampling points leads to spectral leakage in the spectrum, with leaked energy spread throughout the entire f-k domain. Additionally, due to the sampling interval not adhering to the sampling theorem, severe spatial aliasing occurred in linear noise with an apparent velocity of 100 m/s, slight spatial aliasing occurred in linear noise with an apparent velocity of 150 m/s, and no spatial aliasing occurred in linear noise with an apparent velocity of 200 m/s. Due to the sparse and irregular distribution of sampling points, it is difficult to effectively suppress these irregular linear noises using traditional f-k filtering.

In order to measure the denoising performance more clearly, the signal-to-noise ratio (SNR) will be calculated in the following section. The SNR is defined as follows:

$$SNR(dB) = 20log_{10}\frac{\| S \|_2}{\| S - Den \|_2}, \quad (5)$$

where S denotes the noise-free signal data and Den represents the denoised data.

The denoised data and the corresponding removed linear noise are presented in Figure 8. Figure 8a,d express the denoising performance of the filtering method based on radon transform; we can see that a large amount of linear noise is left in the denoised data. The energy of the linear noise is also quite strong in the f-k spectrum, so the method did not suppress the linear noise effectively. The SNR of the denoised result using radon filtering is 9.13. The denoising performance of the traditional f-k filtering method, shown in Figure 8b,e, reveals slight residual linear noise in the denoised data. Additionally, the f-k spectrum indicates that this remaining noise is primarily composed of spatial aliasing and spectral leakage. The SNR of the denoised result using traditional f-k filtering is 14.01. In contrast, Figure 8c,f illustrate the denoising performance of the proposed anti-aliasing and anti-leakage f-k filtering method, which effectively removes the linear noise, leaving only the energy of the effective signal in the f-k spectrum. The highest SNR was obtained using the anti-aliasing and anti-leakage f-k filtering method for denoising, with a result of 21.69. Therefore, the proposed anti-aliasing and anti-leakage f-k filtering method demonstrates greater effectiveness in addressing linear noise suppression in irregular coarse data.

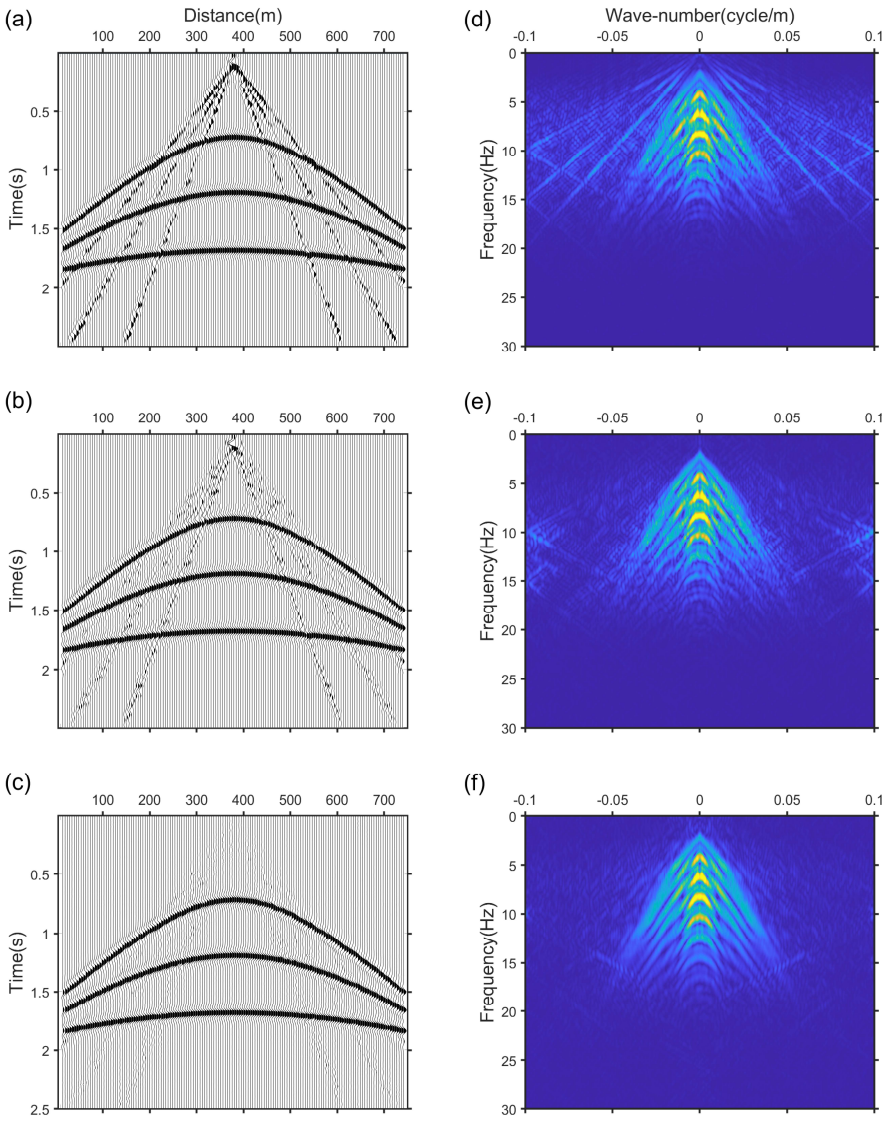


Figure 8. Denoising comparison of synthetic irregular seismic data: (**a**–**c**) denoised results using radon filtering, traditional f-k filtering, and anti-aliasing and anti-leakage f-k filtering, respectively, and (**d**–**f**) anti-leakage Fourier transform spectrum of denoised results using radon filtering, traditional f-k filtering, and anti-aliasing and anti-leakage f-k filtering, respectively.

The corresponding removed linear noise is shown in Figure 9. Figure 9a shows the linear noise removed using the radon filtering. As seen, this method is unable to fully suppress linear noise. This suggests that the radon filtering method can only suppress the dominant energy of linear noise of irregular seismic data but is ineffective in addressing the discontinuities caused by irregular acquisition. Figure 9b illustrates the linear noise removed using the traditional f-k filtering method, since this method does not account for spectral leakage and aliasing issues in irregular coarse seismic data, it can only suppress the dominant linear noise energy. Compared to the linear noise in the original data, the discontinuous characteristics caused by irregularity are also absent in the removed linear noise, which instead appears as smooth and continuous linear noise. Moreover, since the traditional f-k method cannot handle aliased frequencies, the frequency of the removed linear noise is lower compared to that removed by the anti-aliasing and anti-leakage f-k filtering method. In contrast, the anti-aliasing and anti-leakage f-k filtering method preserves the discontinuous features caused by irregular acquisition in the removed linear noise, as shown in Figure 9c. Additionally, the profile of the linear noise removed using

traditional f-k filtering shows slight remnants of the primary signals, as seen in the 1–1.5 s range of the first primary in Figure 9b. We believe this is due to the leakage energy of the Fourier coefficients corresponding to the primaries being removed during spectrum cutting.

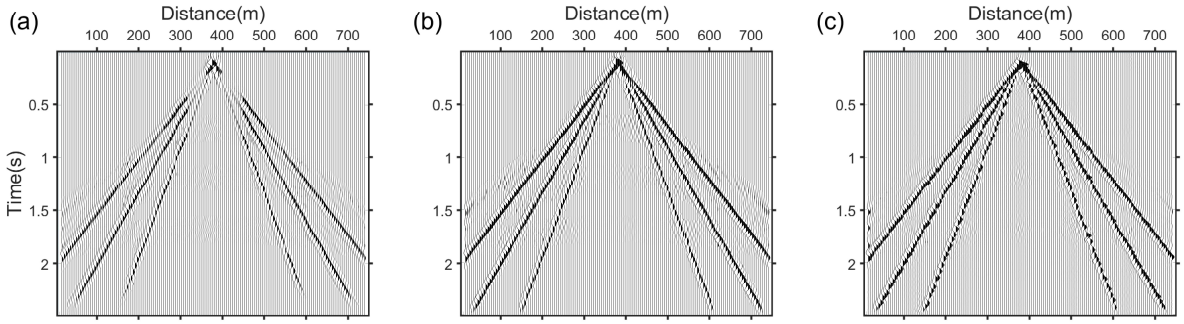


Figure 9. Linear noise removed using (**a**) radon filtering, (**b**) traditional f-k filtering, and (**c**) anti-aliasing and anti-leakage f-k filtering, respectively.

3.2. Deposit Synthetic Data

The second synthetic data example is generated by simulating the Half Mile Lake deposit model proposed by Bellefleur et al. [35]. This ore deposit, located in New Brunswick, Canada, is a volcanic-hosted massive sulfide deposit [36]. To introduce linear noise into the simulated data, we modified the shallow velocity structure by adding a layered low-velocity medium to the near-surface layer; the P-wave velocity range of the low-velocity layer is between 3000 and 5700 m/s, with a thickness of 100 m. Corresponding modifications were made to the S-wave velocity and density. Although this may seem somewhat unreasonable, our goal is to simulate strong surface wave energy. As a result, the parameter settings do not fully align with real-world conditions, making this a somewhat atypical case. To better highlight the surface structure, the specific structure of the low-velocity layer was not detailed in the model; the P-wave velocity section is illustrated in Figure 10. To obtain the irregular seismic data, we designed an irregular geometry with an average sampling interval of 15 m. The synthetic irregular seismic data for the Half Lake deposit model, shown in Figure 11, clearly demonstrate strong surface wave energy with distinct dispersion characteristics.

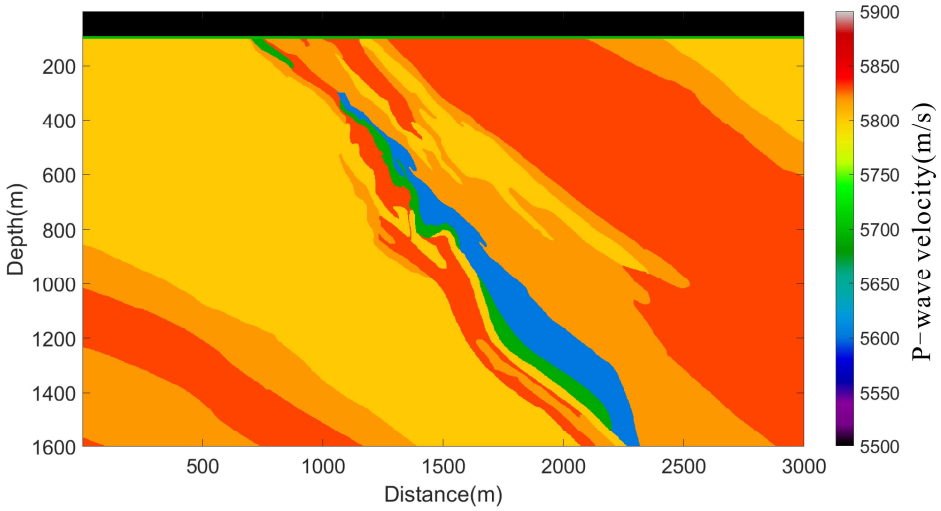


Figure 10. Two-dimensional P-wave velocity section of the Half Mile Lake deposit model.

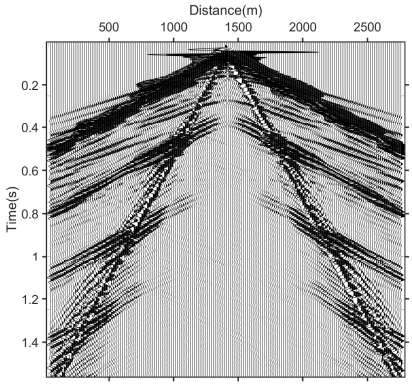


Figure 11. Synthetic irregular seismic data of the Half Mile Lake deposit model with surface wave noise.

Figure 12 shows the denoising results obtained from radon filtering, traditional f-k filtering, and anti-aliasing and anti-leakage f-k filtering, along with the corresponding linear noise removed by each method. The radon filtering method can suppress most of the linear noise, but it also removes a certain amount of the effective signal, which is detrimental to the subsequent seismic data processing results, as shown in Figure 12a,d. Figure 12b,e illustrate the denoised result and corresponding removed linear noise using traditional f-k filtering; it is evident that the method has significantly suppressed the linear noise in the irregular data, but a small amount of high-frequency noise remains unfiltered. In contrast, the anti-aliasing and anti-leakage f-k filtering method's performance is even better, effectively suppressing surface waves with different apparent velocities without damaging the effective signal, as shown in Figure 12c,f.

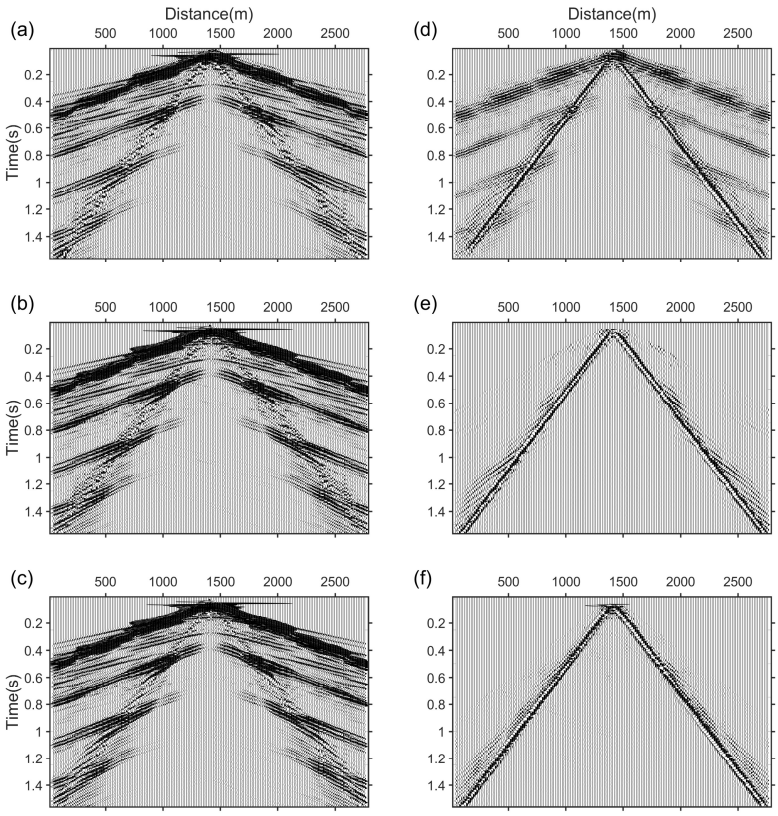


Figure 12. Denoising comparison of the synthetic irregular seismic data of the Half Mile Lake deposit model: (**a**–**c**) denoised results using radon filtering, traditional f-k filtering, and anti-aliasing and anti-leakage f-k filtering, respectively, and (**d**–**f**) removed surface wave noise using radon filtering, traditional f-k filtering, and anti-aliasing and anti-leakage f-k filtering, respectively.

3.3. Land Field Data

The first field seismic data example is a shot gather, as shown in Figure 13. To validate the imaging performance of compressive sensing seismic exploration, seismic data acquisition was conducted in eastern China. The shot and receiver points were randomly and sparsely distributed, using an orthogonal geometry system. A total of 2488 shots were fired, with 18 receiver lines and 6485 geophones arranged for full permutation reception. The seismic source was vibroseis, and the receivers were nodal geophone. Our objective is to remove the surface wave, which is a common type of linear noise in land seismic data. Surface waves are characterized by their linear distribution, high amplitude, low frequency, and low velocity [37]. These waves can significantly impact the effective reflection in the middle and deep layers, resulting in a low SNR of seismic data.

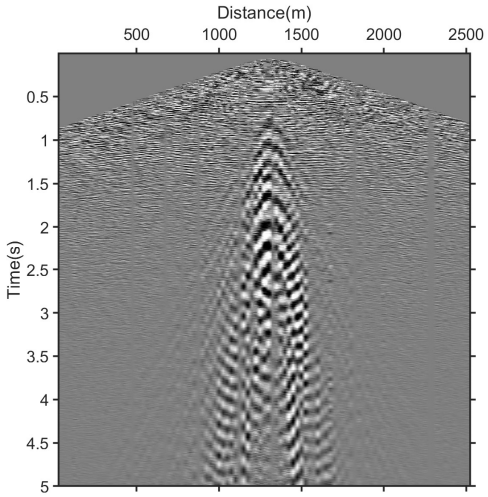


Figure 13. Irregular land field seismic data with surface wave noise.

During data acquisition in this work area, the shot and receiver points were irregularly and sparsely distributed. Consequently, surface waves with lower apparent velocities exhibit a degree of spatial aliasing and spectral leakage in their f-k domain. We applied radon filtering, traditional f-k filtering, and the anti-aliasing and anti-leakage f-k filtering method to suppress the surface waves, with the denoised results and the removed noise presented in Figure 14. In this example, the radon filtering method removes most of the surface wave energy, but it is unable to suppress the surface wave energy corresponding to the spatial aliasing. Traditional f-k filtering also successfully suppresses most surface wave noise but leaves some residual noise. This part of the noise has an opposite dip to the removed noise, which is due to coarse spatial sampling resulting in spatial aliasing and therefore cannot be effectively suppressed by the traditional f-k method. In contrast, anti-aliasing and anti-leakage f-k filtering effectively suppress surface wave noise, resulting in a denoised shot gather with almost no surface wave noise. Thus, for seismic data acquired irregularly and sparsely, anti-aliasing and anti-leakage f-k filtering effectively addresses the challenges of spatial aliasing and spectral leakage, significantly attenuating linear noise.

3.4. Marine Field Data

The second field data example is marine cable seismic data, as shown in Figure 15. The data acquisition was conducted offshore in Tanggu, China, using a 3D marine seismic survey. The survey employed a single-vessel towed cable method with 16 cables, each 6 km in length. The seismic source was an air gun, and the receivers were marine towed cables. The raw data contain various external source noises with negative apparent velocities, which complicate subsequent seismic data processing and interpretation. During this

acquisition, some geophones were damaged, and the useful data obtained were irregular, leading to irregular useful data and the loss of certain linear features of these external noise sources. As with the previous example, radon filtering, traditional f-k filtering, and the anti-aliasing and anti-leakage f-k filtering method were applied to suppress the linear noise.

Figure 16 displays the denoised results obtained from radon filtering, traditional f-k filtering, and the anti-aliasing and anti-leakage f-k filtering method along with the corresponding removed linear noise. It is clear that the radon filtering method has suppressed a large portion of the linear noise, but it has a notable side effect: some of the effective signal is also removed along with the noise. We can also see that traditional f-k filtering leaves some linear noise in the raw data, mainly high-frequency aliasing noise. The anti-aliasing and anti-leakage f-k filtering method achieved the best results in this example. The linear noise energy suppressed by anti-aliasing and anti-leakage f-k filtering is nearly identical to that removed by the radon transform. However, it is worth noting that the anti-aliasing and anti-leakage f-k filtering method has minimal impact on the effective signal, which is crucial for subsequent seismic data processing.

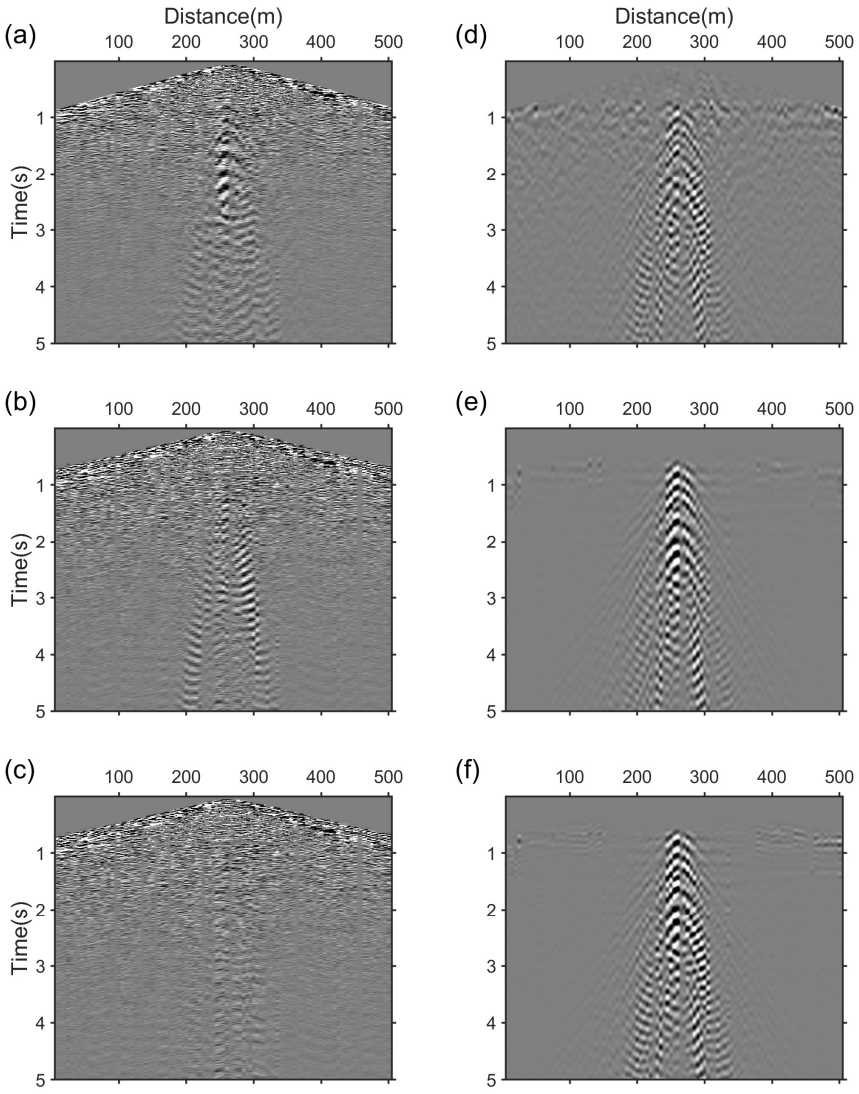


Figure 14. Denoising comparison of the irregular land field seismic data: (**a**–**c**) denoised results using radon filtering, traditional f-k filtering, and anti-aliasing and anti-leakage f-k filtering, respectively, and (**d**–**f**) surface wave noise removed using radon filtering, traditional f-k filtering, and anti-aliasing and anti-leakage f-k filtering, respectively.

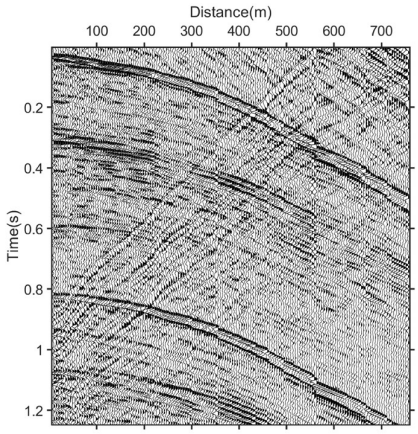


Figure 15. Irregular marine field seismic data with linear noise.

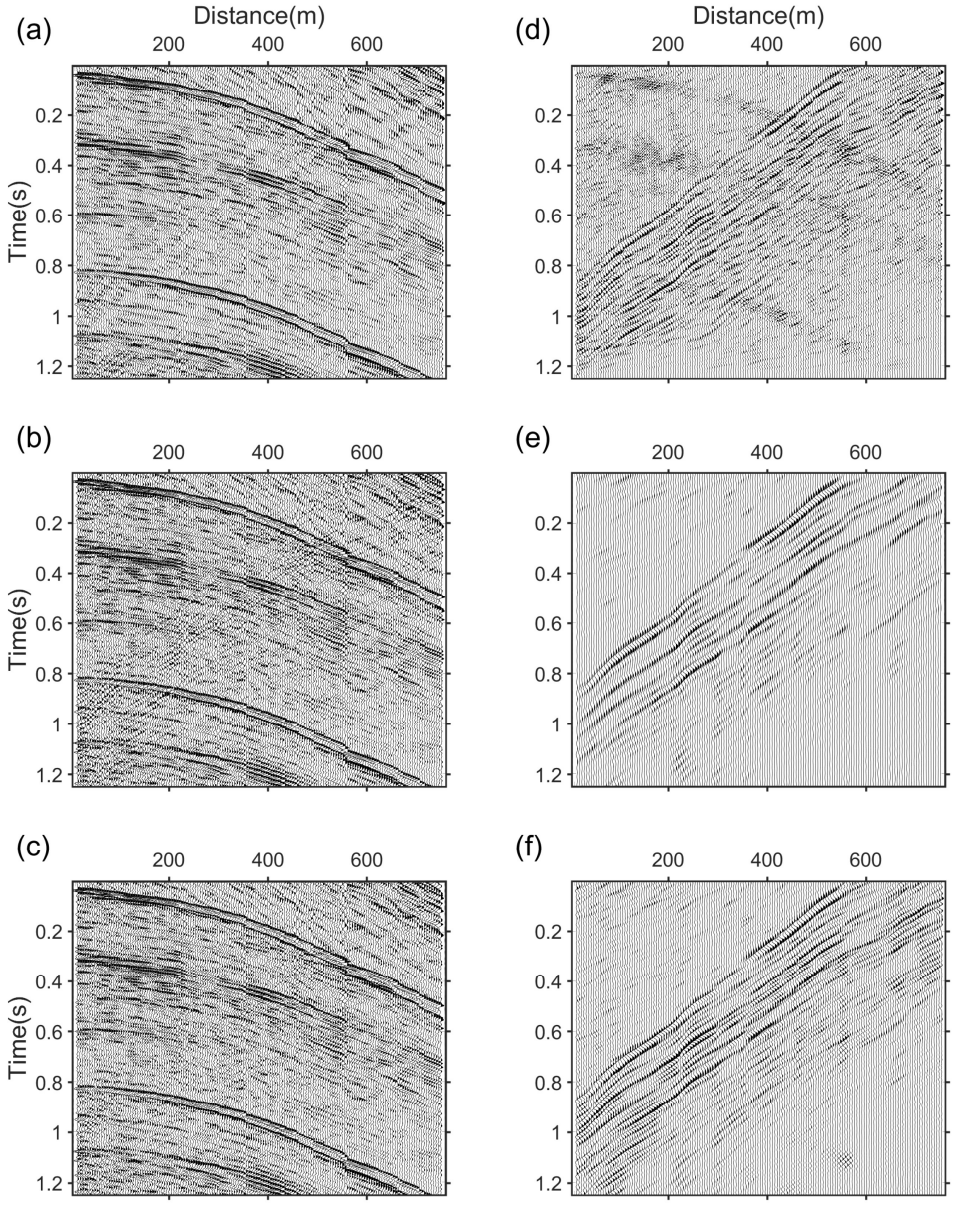


Figure 16. Denoising comparison of the irregular marine field seismic data: (**a**-**c**) denoised results using radon filtering, traditional f-k filtering, and anti-aliasing and anti-leakage f-k filtering, respectively, and (**d**-**f**) removed surface wave noise using radon filtering, traditional f-k filtering, and anti-aliasing and anti-leakage f-k filtering, respectively.

4. Conclusions

To address the challenges of linear noise suppression in irregular coarse seismic data acquisition, we propose the anti-aliasing and anti-leakage f-k filtering method. Existing linear noise suppression methods, due to their theoretical limitations, are ineffective in suppressing linear noise in irregular coarse seismic data, which poses challenges for noise suppression in complex seismic data scenarios. Therefore, we have innovatively proposed, for the first time, a solution to linear noise suppression in irregular coarse seismic data. This method holds promise in overcoming the difficulties of linear noise suppression in seismic data from complex survey areas. This approach integrates linear moveout correction and anti-leakage Fourier transform with traditional f-k filtering. The linear moveout correction component effectively mitigates spatial aliasing issues arising from insufficient sampling, while anti-leakage Fourier transform addresses spectral leakage caused by irregular acquisition, enabling the retrieval of the true spectrum from the irregular data. Both synthetic and field seismic data examples demonstrate that the anti-aliasing and anti-leakage f-k filtering method significantly enhances linear noise suppression in irregular coarse seismic data.

Author Contributions: Conceptualization, S.M.; methodology, S.M.; software, S.M., X.L., L.H., and L.R.; validation, X.L.; formal analysis, L.H.; investigation, G.S.; resources, S.M.; data curation, S.M.; writing—original draft preparation, S.M.; writing—review and editing, S.M., X.L., L.H., L.R., and G.S.; visualization, L.H.; supervision, S.M.; project administration, S.M.; funding acquisition, X.L. All authors have read and agreed to the published version of the manuscript.

Funding: This work is supported by the National Key R&D Program of China (2021YFA0716902, 2022YFB3904601). This work is supported by the national natural science foundation of China under grant no. 41904114, no. 42174160.

Data Availability Statement: The data presented in this study are available on request from the corresponding author due to internal policy.

Conflicts of Interest: Author Liying Ren was employed by the Liaohe Geophysical Exploration Company of BGP CNPC. The remaining authors declare that the research was conducted in the absence of any commercial or financial relationships that could be construed as a potential conflict of interest.

References

1. Merle, A.T.; Howard, E.T.; Pembroke, J.H. Crustal structure from seismic exploration. *J. Geophys. Res.* **1954**, *59*, 415–422.
2. Chen, Y.; Wang, B.S.; Yao, H.J. Seismic airgun exploration of continental crust structures. *Sci. China Earth Sci.* **2017**, *60*, 1739–1751. [CrossRef]
3. Aminzadeh, F.; Dasgupta, S.N. Fundamentals of Petroleum Geophysics. *Dev. Pet. Sci.* **2013**, *60*, 37–92.
4. Abdel, F.H.; Ahmed, I.D.; Mehdi, P.Y.; Hatem, F.E. Improvement of Gulf of Suez subsurface image under the salt layers through re-processing of seismic data—A case study. *NRIAG J. Astron. Geophys.* **2020**, *9*, 38–51. [CrossRef]
5. Siahsar, M.A.; Gholtashi, S.; Kahoo, A.R.; Chen, W.; Chen, Y.K. Data-driven multitask sparse dictionary learning for noise attenuation of 3D seismic data. *Geophysics* **2017**, *82*, V385–V396. [CrossRef]
6. Yilmaz, O. Seismic Data Analysis: Processing, inversion, and interpretation of seismic data. *Soc. Expl. Geophys.* **2001**, *10*, 658–663.
7. Huang, W.L.; Wang, R.Q.; Zhang, D.; Zhou, Y.X.; Yang, W.C.; Chen, Y.K. Mathematical morphological filtering for linear noise attenuation of seismic data. *Geophysics* **2017**, *82*, V369–V384. [CrossRef]
8. Chen, W.; Chen, Y.K.; Liu, W. Ground roll attenuation using improved complete ensemble empirical mode decomposition. *J. Seism. Explor.* **2016**, *25*, 485–495.
9. Wang, W.; Gao, J.H.; Chen, W.C.; Xu, J. Data adaptive ground-roll attenuation via sparsity promotion. *J. Appl. Geophys.* **2012**, *83*, 19–28. [CrossRef]
10. Ge, J.; Magnani, M.B.; Waldron, B. Imaging a shallow aquitard with seismic reflection data in Memphis, Tennessee, USA. Part II: Data analysis, interpretation and traveltime tomography. *Near Surf. Geophys.* **2010**, *8*, 331–340. [CrossRef]
11. Embree, P.; Burg, J.P.; Backus, M.M. Wide-band velocity filtering. *Geophysics* **1963**, *28*, 948–974. [CrossRef]
12. Guo, J.Y. Prestack noise reduction using (ω-x)-domain operator extrapolation. *Oil Geophys. Prospect.* **1995**, *30*, 487–494.

13. Liu, X.W. Ground roll suppression using the Karhunen-Loeve transform. *Geophysics* **1999**, *64*, 564–566. [CrossRef]
14. Henley, D.C. The radial trace transform: An effective domain for coherent noise attenuation and wavefield separation. In *SEG Technical Program Expanded Abstracts 1999*; Society of Exploration Geophysicists: Houston, USA, 1999.
15. Zhu, W.H.; Kelamis, P.G.; Liu, Q.L. Linear noise attenuation using local radial trace median filtering. *Lead. Edge* **2004**, *23*, 728–737. [CrossRef]
16. Lu, W.K.; Zhang, W.; Liu, D. Local linear coherent noise attenuation based on local polynomial approximation. *Geophysics* **2006**, *71*, V163–V169. [CrossRef]
17. Hong, F.; Hu, T.Y.; Wang, R.Q. Using 3D beamforming filtering method to eliminate coherent noise. *Oil Geophys. Prospect.* **2005**, *40*, 42–47.
18. Neelamani, R.; Baumstein, A.I.; Gillard, D.G.; Hadidi, M.T.; Soroka, W.L. Coherent and random noise attenuation using the curvelet transform. *Lead. Edge* **2008**, *27*, 240–248. [CrossRef]
19. Tong, S.Y.; Wang, L.F.; Liu, H.S.; Jin, Z.; Wang, R.Q. Marine Linear Noise Suppression in the Curvelet Domain. In Proceedings of the 2009 International Forum on Information Technology and Applications, Chengdu, China, 15–17 May 2009; IEEE: Piscataway, NJ, USA, 2009.
20. Qin, T. Prestack coherent noise attenuation based on wavelet frequency division. *Prog. Geophys* **2009**, *24*, 1426–1430.
21. Teng, H.H.; Jiao, J.R.; Shang, X.M.; Wang, Y.H.; Zhao, S.T.; Yan, G.; Yang, B.; Zhu, X.H. Two-dimensional complex wavelet transform for linear noise attenuation and image decomposition. *J. Geophys. Eng.* **2023**, *20*, 474–482. [CrossRef]
22. Yan, X.H.; Lu, J.F.; Zhang, X.T. The linear Radon transformation and its application in the northern block of Xinjiang. *Pet. Geophys.* **2011**, *9*, 9–14+19.
23. Ebadi, M.R. Coherent and incoherent seismic noise attenuation using parabolic radon transform and its application in environmental geophysics. *Model. Earth Syst. Environ.* **2017**, *3*, 18. [CrossRef]
24. Zhu, W.Q.; Mousavi, S.M.; Beroza, G.C. Seismic signal denoising and decomposition using deep neural networks. *IEEE Trans. Geosci. Remote Sens.* **2019**, *57*, 9476–9488. [CrossRef]
25. Chen, J.X.; Chen, G.X.; Li, J.; Du, R.S.; Qi, Y.L.; Li, C.F. Efficient Seismic Data Denoising via Deep Learning with Improved MCA-SCUNet. *IEEE Trans. Geosci. Remote Sens.* **2024**, *62*, 5903614. [CrossRef]
26. Ma, X.; Yao, G.; Yuan, S.Y.; Zhang, F.; Wu, D. Seismic Coherent noise removal with residual network and synthetic seismic samples. *IEEE Geosci. Remote Sens. Lett.* **2024**, *21*, 1–5. [CrossRef]
27. Hennenfent, G.; Herrmann, F. Simply denoise: Wavefield reconstruction via jittered undersampling. *Geophysics* **2008**, *73*, V19–V28. [CrossRef]
28. Zhou, S.; Lv, Y.; Lv, G.; Shu, G.; Shi, T.; Huo, S. Irregular seismic geometry design and data reconstruction based on compressive sensing. *Geophys. Prospect. Pet.* **2017**, *56*, 617–625.
29. Sun, Y.H.; Schuster, K.S.; Sikorski, K. A quasi-Monte Carlo approach to 3-D migration: Theory. *Geophysics* **1997**, *62*, 918–928. [CrossRef]
30. Xu, S.; Zhang, Y.; Lambare, G. Antileakage Fourier transform for seismic data regularization in higher dimensions. *Geophysics* **2005**, *75*, WB113–WB120. [CrossRef]
31. Naghizadeh, M.; Sacchi, M.D. On sampling functions and Fourier reconstruction methods. *Geophysics* **2010**, *75*, WB137–WB151. [CrossRef]
32. Jamali-Rad, H.; Kuvshinov, B.; Tang, Z.; Campman, X. Deterministically Subsampled Acquisition Geometries for Optimal Reconstruction. In Proceedings of the 78th EAGE Conference and Exhibition, Vienna, Austria, 30 May–2 June 2016.
33. Shu, G.X.; Lv, G.H.; Lv, Y.; Shi, T.K.; Di, Z.X.; Huo, S.D. Seismic data reconstruction based on compressive sensing. *Geophys. Prospect. Pet.* **2018**, *57*, 549–554.
34. Zwartjes, P.M.; Sacchi, M.D. Fourier reconstruction of nonuniformly sampled, aliased seismic data. *Geophysics* **2007**, *72*, V21–V32. [CrossRef]
35. Bellefleur, G.; Malehmir, A.; Müller, C. Elastic finite-difference modeling of volcanic-hosted massive sulfide deposits: A case study from Half Mile Lake, New Brunswick, Canada. *Geophysics* **2012**, *77*, WC25–WC36. [CrossRef]
36. Adair, R.N. Stratigraphy, structure, and geochemistry of the Halfmile Lake massive-sulfide deposit, New Brunswick. *Explor. Min. Geol.* **1992**, *1*, 151–166.
37. Sheriff, R.E.; Geldart, L.P. *Exploration Seismology*; Cambridge University Press: Cambridge, UK, 1995.

Disclaimer/Publisher's Note: The statements, opinions and data contained in all publications are solely those of the individual author(s) and contributor(s) and not of MDPI and/or the editor(s). MDPI and/or the editor(s) disclaim responsibility for any injury to people or property resulting from any ideas, methods, instructions or products referred to in the content.